# Journal Pre-proof


Design, synthesis and evaluation of liposomes modified with dendritic aspartic acid for bone-specific targeting

Ze Zhao, Changqing Chen, Changwei Xie, Yi Zhao

PII: S0009-3084(19)30197-5

DOI: https://doi.org/10.1016/j.chemphyslip.2019.104832

Reference: CPL 104832

To appear in: *Chemistry and Physics of Lipids*

Received Date: 9 August 2019

Revised Date: 9 September 2019

Accepted Date: 21 September 2019

Please cite this article as: Zhao Z, Chen C, Xie C, Zhao Y, Design, synthesis and evaluation of liposomes modified with dendritic aspartic acid for bone-specific targeting, *Chemistry and Physics of Lipids* (2019), doi: https://doi.org/10.1016/j.chemphyslip.2019.104832

# Design, synthesis and evaluation of liposomes modified with dendritic aspartic acid for bone-specific targeting

Ze Zhao[a,*], Changqing Chen[a], Changwei Xie[a], Yi Zhao[b,*]

[a] *Department of Orthopedics, the First Affiliated Hospital of Henan Polytechnic University (the Second People's Hospital of Jiaozuo City), Jiaozuo 454001, China.*

[b] *Department of Translational Medicine Center, the First Affiliated Hospital of Zhengzhou University, Zhengzhou 450052, China*

*Corresponding authors. zezhao0910@163.com (Z. Zhao), zhaoyi0910@163.com (Y. Zhao)

Graphic Abstract

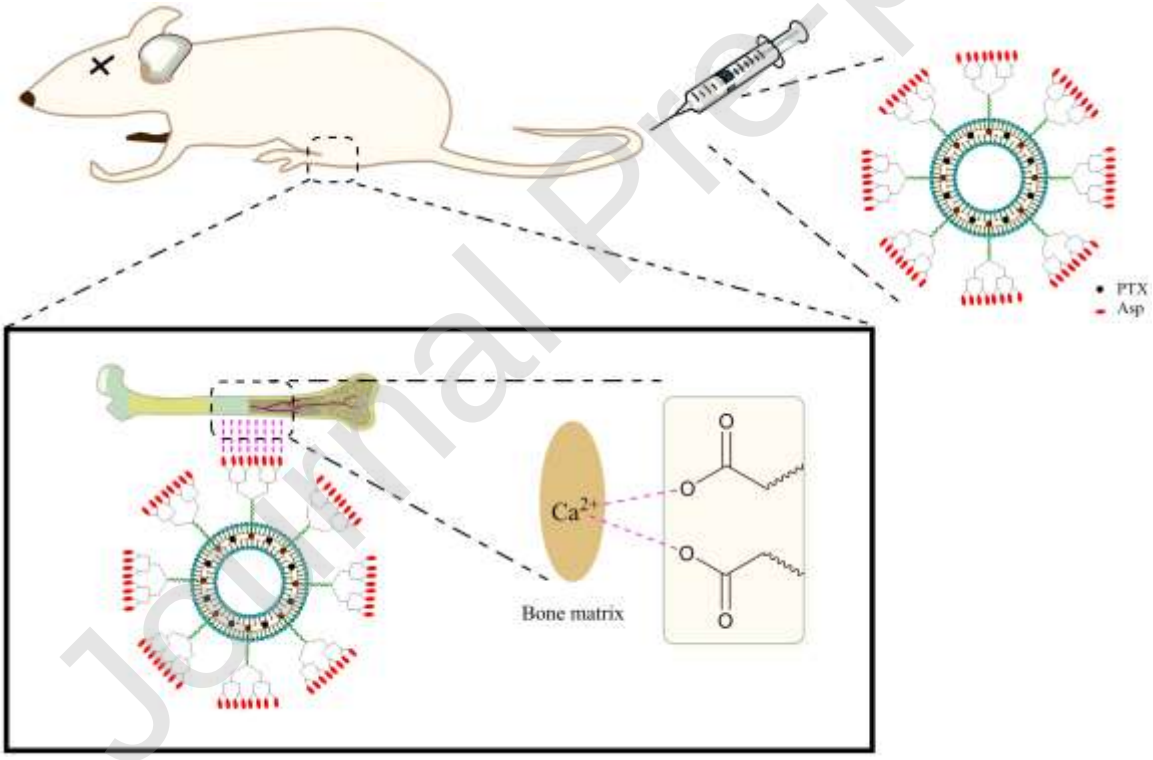


Highlights

- A series of novel dendritic aspartic acid derivatives were designed and synthesized as liposome

ligands.

- The preliminary evaluation *in vivo* demonstrated that ligand $Asp_8$-coated liposome had an improved bone-targeting ability.
- The quantity of Asp residues will increase the affinity for bone.


## Abstract

Bone diseases are notoriously difficult diseases to treat due to the comparatively low blood flows in bone tissue. Therefore, targeting delivery of drugs to bone may not only enhance the treatment efficacy, but also reduce the quantity of drug administered. In order to increase the distribution of paclitaxel (PTX) in bone, in this study, a series of novel dendritic aspartic acid derivatives were designed and synthesized as liposome ligands to deliver PTX to bone effectively. The liposomes were prepared by thin film hydration method and its particle size, zeta potential, encapsulation efficiency, release profile, stability, hemolysis were also characterized. All the aspartic acid-coated liposomes showed more than 60% binding rates to hydroxyapatite (HAP), especially the PTX-$Asp_8$-Lip exhibited dramatic binding rates (> 97%) after 24 h. Moreover, the bone-targeting study *in vivo* indicated that all liposomes could improve the accumulation of PTX in bone, among which, the PTX-$Asp_8$-Lip showed the best affinity due to the increase of aspartic acid residues exposed on the liposome surface. These results provided a novel and effective entry to the development of bone-targeting drugs.


**Keywords**: Drug delivery, Bone targeting, Dendritic aspartic acid, Liposome

## 1. Introduction

Bone diseases, such as bone metastasis, osteomyelitis, osteoporosis, Paget's disease, are notoriously difficult diseases to treat due to the comparatively low blood flows in bone tissue [Chastain and Davis, 2019; Zhao et al., 2015; Zhao et al., 2019]. Among them, bone metastasis is a frequent complication in advanced stage of many cancers, especially breast, prostate, and lung cancers [Sun et al., 2019]. It could give rise to bone pain, hypercalcemia, pathological fracture and bone malformation because of the increased activity of osteoclast cells, which leads to the decrease of life quality [Yamashite et al., 2018]. Current treatments for metastatic bone cancers mainly are surgery, radiotherapy and chemotherapy, or the

combination of them. Although the chemotherapy has played an important role in increasing the survival rate and improving the life quality of patients, its low targeting efficiency makes the high and frequent administration essential, which may lead to severe side effects [Yamashite et al., 2018; Zhao et al., 2019]. Therefore, there is a huge amount of demand of specific delivery systems of chemotherapeutic agents, such as paclitaxel (PTX), to the site of bone lesions are of great interests for the treatment of metastatic bone cancer.

To overcome the limitations of chemotherapy for treating bone metastasis, bone-targeting drug delivery is a promising solution to increase therapeutic efficiency and severe side effects. As we all know, bone is consist of some unique materials, and the inorganic compound hydroxyapatite (HAP) is the major ingredient of bone, which is a potential target for selective drug delivery to bone [Zhao et al., 2019]. In our previous study, we have found that dendritic aspartic acid (Asp) derivatives had an excellent bone-targeting abilities [Pan et al., 2012]. According to Sarig's research, the mechanisms for the bone-affinity of Asp oligopeptides is that the multi-carboxy groups of peptides provide ionic interaction between negative charges and calcium ions in the mineral component of bone (HAP), and this kind of affinity only depends on the number of exposed amino acid residues [Sarig 2004]. Simultaneously, we assumed that the more the quantity of Asp residues exposed on the liposome surface, the stronger the affinity for bone showed.

With the development of macromolecules, dendrimers, consisting of two dendrons, are widely used in medical and biomedical fields such as drug delivery [Pan et al., 2012]. Over the years, we has done many researches on bone targeting or dendrimers specially based on acidic peptides [Pan et al., 2012; Zhao et al., 2015; and Zhao et al., 2019]. The acidic peptides are biodegradable, biocompatible, and has shown strong affinity to bone. And we are still exploring how to further improve the carrier's bone targeting ability to deliver more drugs to bone.

As a drug carrier, liposome has many advantages such as nontoxicity, biocompatibility and biodegradability, which is widely applied in drug delivery system [Matsuo et al., 2019]. Inspired by the affinity mechanism and the dendritic effect, we developed a series of novel dendritic aspartic acid derivatives (Fig. 1) as ligands to increase the quantity of negatively charged groups (carboxy groups of Asp) exposed on the liposome surface. Using post-insertion technique, the lipophilic steroidal portion was embedded into the liposome membrane, while the hydrophilic dendritic Asp residues were exposed outside the membrane. The dendritic Asp-modified liposomes were prepared by the lipid film hydration-ultrasound

method. What's more, to investigate the bone targeting ability, the targeting ability *in vitro* and *in vivo* was evaluated.

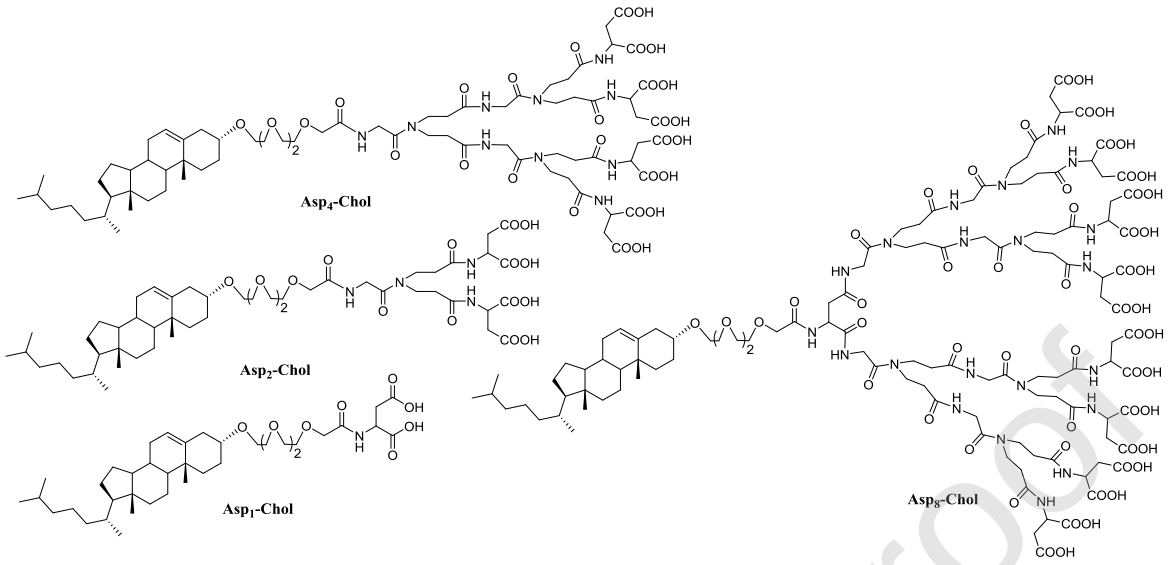


**Figure 1**. The structure of dendritic Asp-modified ligand $Asp_1$-Chol, $Asp_2$-Chol, $Asp_4$-Chol, and $Asp_8$-Chol.

## 2. Materials and methods

### *2.1. Materials*

All unspecified reagents were from commercial resources. TLC was performed using precoated silica gel GF254 (0.2 mm), while column chromatography was performed using silica gel (100-200 mesh). Elemental analyses were performed by Atlantic Microlab (Atlanta, GA, USA). Reversed-phase chromatography performed on C18 chromatographic analysis was carried out using the HPLC system (Alltech, IL, USA) consisted of a RF-530 fluorescence detector (Shimadzu, Japan) and Allchorom plus data operator, respectively. A Diamonsil column (200 × 4.6 mm, 5 μm) was used. Soybean phospholipids (SPC) were purchased from Shanghai Taiwei Chemical Company (Shanghai, China). Paclitaxel (PTX) was purchased from AP Pharmaceutical Co. Ltd. (Chongqing, China).

### *2.2. Methods*

#### *2.2.1 Chemistry*

##### *2.2.1.1 Synthesis of compound **3-13***

The synthesis of compound **3-13** was reported in our previous work [Pan et al., 2012; Zhao et al., 2014; Zhao et al., 2015; Zhao et al., 2018; and Zhao et al., 2019].

##### *2.2.1.2 Synthesis of compound **14***

To a solution of compound **13** (1.50 g, 2.60 mmol) in $CH_2Cl_2$ (30 mL) were added isobutyl chloroformate (IBCF, 0.43 mL, 3.38 mmol) and 4-methylmorpholine (NMM, 0.43 mL, 3.90 mmol), then

the mixture was stirred at -15 °C for 20 min. Subsequently, Asp(OBn)-OBn (1.14 g, 3.64 mmol) in $CH_2Cl_2$ (10 mL) was added to the above reaction mixture slowly and the reaction was continued to stir for 5 h at room temperature. The reaction was terminated and then filtered. The filtrate was washed with 1 M HCl (20 mL), 1 M $NaHCO_3$ (20 mL), and brine (20 mL). The organic layer was dried over sodium sulfate, filtered, concentrated under reduced pressure and purified by silica gel column chromatography to give compound **14** (1.90 g, 84%) as colorless oil. ESI-MS (m/z): calculated for $C_{53}H_{77}NO_9Na$ $[M+Na]^+$ 894.5496, found 894.5490. Elemental Analysis: C, 72.99; H, 8.90; N, 1.61, found C, 72.85; H, 9.01; N, 1.73.

*2.2.1.3 Synthesis of ligand Asp₁-Chol*

The mixture of **14** (1.22 g, 1.40 mmol) and 10% Pd/C (0.12 g) in methanol (15 mL) was stirred at the room temperature under hydrogen atmosphere. After 2 h, the mixture was filtered, and the filtrate was concentrated to obtain ligand $Asp_1$-Chol (0.90 g, 93%) as colorless oil. ESI-MS (m/z): calculated for $C_{39}H_{65}NO_9Na$ $[M+Na]^+$ 714.4557, found 714.4552. Elemental Analysis: C, 67.70; H, 9.47; N, 2.02, found C, 67.79; H, 9.38; N, 2.11.

*2.2.1.4 Synthesis of compound **15***

To a solution of $Asp_1$-Chol (0.45 g, 0.65 mmol) in $CH_2Cl_2$ (20 mL) were added IBCF (0.11 mL, 0.85 mmol) and NMM (0.11 mL, 0.98 mmol), then the mixture was stirred at -15 °C for 20 min. Subsequently, compound **8** (2.92 g, 1.63 mmol) in $CH_2Cl_2$ (20 mL) was added to the above reaction mixture slowly and the reaction was continued to stir for 24 h at room temperature. The reaction was terminated and then filtered. The filtrate was washed with 1 M HCl (30 mL), 1 M $NaHCO_3$ (30 mL), and brine (30 mL). The organic layer was dried over $Na_2SO_4$, filtered, concentrated under reduced pressure and purified by silica gel column chromatography to give compound **15** (1.58 g, 57%) as colorless oil. MALDITOF-MS (m/z): calculated for $C_{231}H_{273}N_{21}O_{57}Na$ $[M+Na]^+$ 4277.907, found 4277.911. Elemental Analysis: C, 65.19; H, 6.47; N, 6.91, found C, 65.05; H, 6.59; N, 6.79.

*2.2.1.5 Synthesis of ligand Asp₈-Chol*

The mixture of **15** (1.00 g, 0.23 mmol) and 10% Pd/C (0.10 g) in methanol (20 mL) was stirred at the room temperature under hydrogen atmosphere. After 20 h, the mixture was filtered, and the filtrate was concentrated to obtain ligand $Asp_8$-Chol (0.56 g, 85%) as colorless oil. MALDITOF-MS (m/z): calculated for $C_{119}H_{177}N_{21}O_{57}Na$ $[M+Na]^+$ 2836.153, found 2836.157. Elemental Analysis: C, 50.80; H, 6.34; N, 10.45, found C, 50.92; H, 6.44; N, 10.32.

*2.2.1.6 Synthesis of compound **16***

Compound **13** (0.92 g, 1.59 mmol) was dissolved in $CH_2Cl_2$ (30 mL) and was cooled at -15 °C. Then, IBCF (0.28 mL, 2.23 mmol) and NMM (0.26 mL, 2.39 mmol) were added, and the mixture was stirred for 15 min. Subsequently, compound **8** (3.43 g, 1.91 mmol) in $CH_2Cl_2$ (20 mL) was added dropwise to the reaction and the mixture was vigorously stirred for another 24 h at room temperature. The reaction was terminated and then filtered. The filtrate was washed with 1 M HCl (30 mL), 1 M $NaHCO_3$ (30 mL), and brine (30 mL). The organic layer was dried over $Na_2SO_4$, filtered, concentrated under reduced pressure and purified by silica gel column chromatography to give compound **16** (2.48 g, 66%) as colorless oil. MALDITOF-MS (m/z): calculated for $C_{131}H_{164}N_{10}O_{30}Na$ $[M+Na]^+$ 2381.155, found 2381.150. Elemental Analysis: C, 66.71; H, 7.01; N, 5.94, found C, 66.79; H, 7.10; N, 5.86.

*2.2.1.7 Synthesis of ligand $Asp_4$-Chol*

10% Pd/C (0.20 g) was added into the solution of compound **16** (0.26 g, 0.11 mmol) in methanol (10 mL). The reaction mixture was stirred at the room temperature under hydrogen atmosphere for 20 h, then filtered. The filtrate was concentrated to obtain ligand $Asp_4$-Chol (0.16 g, 91%) as colorless oil. MALDITOF-MS (m/z): calculated for $C_{75}H_{116}N_{10}O_{30}Na$ $[M+Na]^+$ 1659.776, found 1659.773. Elemental Analysis: C, 55.00; H, 7.14; N, 8.55, found C, 55.13; H, 7.25; N, 8.45.

*2.2.1.8 Synthesis of compound **17***

To a solution of compound **13** (1.44 g, 2.50 mmol) in $CH_2Cl_2$ (20 mL) were added IBCF (0.44 mL, 3.50 mmol) and NMM (0.41 mL, 3.74 mmol), then the mixture was stirred at -15 °C for 20 min. Subsequently, compound **6** (2.43 g, 3.00 mmol) in $CH_2Cl_2$ (15 mL) was added to the above reaction mixture slowly and the reaction was continued to stir for 15 h at room temperature. The reaction was terminated and then filtered. The filtrate was washed with 1 M HCl (20 mL), 1 M $NaHCO_3$ (20 mL), and brine (20 mL). The organic layer was dried over sodium sulfate, filtered, concentrated under reduced pressure and purified by silica gel column chromatography to give compound **17** (2.66 g, 78%) as colorless oil. ESI-MS (m/z): calculated for $C_{79}H_{106}N_4O_{16}Na$ $[M+Na]^+$ 1389.7502, found 1389.7506. Elemental Analysis: C, 69.38; H, 7.81; N, 4.10, found C, 69.46; H, 7.94; N, 4.17.

*2.2.1.9 Synthesis of ligand $Asp_2$-Chol*

To a solution of compound **17** (1.69 g, 1.24 mmol) in $CH_3OH$ (20 mL), Pd/C (0.20 g, 10%) was added. Then, the mixture was stirred in hydrogen atmosphere at r.t. for 10 h. Pd/C was filtered, and the filtrate was concentrated to give ligand $Asp_2$-Chol (1.12 g, 90%) as colorless oil. ESI-MS (m/z): calculated for

$C_{51}H_{82}N_4O_{16}Na$ $[M+Na]^+$ 1029.5624, found 1029.5627. Elemental Analysis: C, 60.82; H, 8.21; N, 5.56, found C, 60.95; H, 8.07; N, 5.64.

*2.2.2 Preparation and characterization of liposomes*

PTX-loaded liposomes were prepared through thin film hydration method as our previous reported [Zhao et al., 2019], including a main lipid composition of SPC, cholesterol, and synthesized ligands. The component ratio optimized according to our previous report was as follows: (1) uncoated Lip, SPC/cholesterol/: 62/33; (2) $Asp_1$-Lip, SPC/cholesterol/$Asp_1$-Chol: 62/33/3; (3) $Asp_2$-Lip, SPC/cholesterol/$Asp_2$-Chol: 62/33/3; (4) $Asp_4$-Lip, SPC/cholesterol/$Asp_4$-Chol: 62/33/3; (5) $Asp_8$-Lip, SPC/cholesterol/$Asp_8$-Chol: 62/33/3. In brief, the lipid materials were dissolved in the chloroform/methanol (v/v = 2:1), and then dried using a rotary evaporator at 37 °C, which was further dried in vacuum for 24 h. Subsequently, the dried thin film was hydrated with PBS (pH 7.4) at 20 °C for 0.5 h and then sonicated intermittently by a probe sonicator at 80 W for 80 s to form liposomes.

To prepare PTX-loaded liposomes, appropriate amount of paclitaxel was added into the lipid organic solution prior to the solvent evaporation. Detections about entrapment efficiency (EE%) and drug loading efficiency (DL%) were conducted using high performance liquid chromatography (HPLC). Measurement was performed on a LC-10A liquid chromatographic system (Shimadzu). The analytical column was a reverse-phase HPLC column (ODS-C18 column, 4.6mm × 200 mm, 5 μm, SinoChrom) maintaining at 30 °C. The mobile phase consisted of water-methanol (67:33, v/v) with a low flow rate 1.0 mL/min. The sample volume injected was 20 μL and the detection wavelength was 227 nm. The EE% and DL% were calculated using the following equations: EE% = weight of encapsulated PTX / the total weight of PTX, DL% = weight of encapsulated PTX / the total weight of PTX-loaded liposome. The particle size and zeta potential of Lip, $Asp_1$-Lip, $Asp_2$-Lip, $Asp_4$-Lip, and $Asp_8$-Lip were characterized by Malvern Zeta sizer Nano ZS90 (Malvern Instruments Ltd., UK).

*2.2.3 In vitro paclitaxel release study of liposomes*

The paclitaxel release analysis from PTX-loaded liposomes was performed in PBS (pH 7.4) using dialysis method. Briefly, each PTX liposomal formulation (0.4 mL) and free paclitaxel were put into a dialysis bag (MWCO = 8 000 – 14 000 Da) placed in 40 ml release medium (PBS containing 0.1% (v/v) Tween 80). It was gently oscillated at 37 °C and 0.1 mL sample was taken out and replaced with fresh medium at predetermined time points (0 h, 1 h, 2 h, 4 h, 8 h, 12 h, 24 h and 48 h). Then, the amount of PTX was determined using HPLC method as mentioned above.

*2.2.4 Stability of liposomes*

To investigate the stability of PTX liposomal formulations, the turbidity variations in the presence of fetal bovine serum (FBS) and the appearance In brief, 0.1 mL PTX-loaded liposome was incubated in FBS (0.1 mL) with moderate shaking (45 rpm) at 37 °C. The transmittance of each sample was detected at the predetermined time points (0 h, 1 h, 2 h, 4 h, 8 h, 12 h, 24 h and 48 h) using a microplate reader (Thermo Scientific Varioskan Flash, USA) at 750 nm. What's more, the stability of liposomes stored at 4 °C for several days was also investigated by monitoring their particle size and polydispersity index (PDI) at the predetermined time points.

*2.2.5 Hemolysis assays*

For hemolysis assays, the mouse red blood cells (MRBCs) were obtained according to our previous report [Zhao et al., 2019]. Briefly, the fresh mouse blood was stabilized and centrifuged at $5 \times 10^3$ rpm for 5 min to remove the supernatant. Afterwards, the precipitated MRBCs were washed with PBS, and then diluted with PBS to a concentration of 2% (w/v). Subsequently, 0.1 mL MRBCs solution was added into different liposomes with 0.4 mL various concentrations of lipids (10-400 nM). MRBCs incubated with PBS and Triton X-100 were utilized as negative and positive controls, respectively. All the mixtures were incubated at 37 °C for 2 h with gentle shaking, and were centrifuged at $1 \times 10^4$ rpm for 10 min. Finally, the absorbance of the supernatant was measured using a microplate reader (Thermo Scientific Varioskan Flash) at 540 nm. The hemolytic activity percentages of the different samples were calculated using the following equation: the percent hemolysis (%) = $(A_{Sample}-A_{Negative})/(A_{Postive}-A_{Negative}) \times 100\%$, where A is the absorbance of hemoglobin.

*2.2.6 Hydroxyapatite binding assay*

The hydroxyapatite binding assay of these dendritic aspartic acid-modified liposomal formulations toward bone matrix was conducted according to our previously reported procedure [Zhao et al., 2015; Zhao et al., 2019]. In brief, the hydroxyapatite was dissolved in PBS at the concentration of 20 mg/mL. Then, 0.3 mL PTX-Lip, PTX-$Asp_1$-Lip, PTX-$Asp_2$-Lip, PTX-$Asp_4$-Lip, PTX-$Asp_8$-Lip, and free PTX (calculated as PTX) were respectively incubated with 0.3 mL HAP suspension and shaken gently at 37 °C. At the same time, these liposomes were incubated in PBS without HAP used as negative control. At the predetermined time (0.5 h, 1 h, 2 h, and 24 h), the unbound PTX was separated from the mixture by centrifugation at 5000 rpm for 3 min. Afterwards, the unbound PTX in the supernatant was determined quantificationally through HPLC. The binding efficiency was calculated by HAP binding rate (%) =

$(C_0\text{-}C)/C_0$.

*2.2.7 Cytotoxicity assay*

*In vitro* cytotoxicity of the synthetic ligands ($Asp_1$-Chol, $Asp_2$-Chol, $Asp_4$-Chol, and $Asp_8$-Chol) was measured on MDA-MB-231 cells using MTT assay. Generally, the cells were seeded into a 96-well plate at a density of $5 \times 10^3$ cells/well, and incubated in a 5% $CO_2$ humidified environment incubator (Thermo Scientific, USA) at 37 °C for 24 h. After that, the blank liposomes (PTX-unloaded) contained in fresh medium were added at different concentrations. After 24 h incubation, 20 μL of MTT solution (5.0 mg/mL) was added to each well and the cells were cultured for another 4 h at 37 °C. Then, the medium were removed and the dye was dissolved in DMSO (150 μL). The amount of absorption in each well reflects the conversion of MTT to formazan by metabolically viable cells, and the cell viability was calculated using the following equation: $A_{Sample}$ / $A_{Control}$ × 100%, where $A_{Sample}$ and $A_{Control}$, where $A_{Sample}$ and $A_{Control}$ represent the absorbance of sample cells and control cells read at 490 nm on an automatic microplate spectrophotometer, respectively.

*2.2.8 Pharmacokinetic study*

Pharmacokinetic study was conducted on healthy Sprague Dawley (SD) rats and the concentration of PTX was determined by HPLC as described previously. Briefly, SD rats (180-220 g) were randomly divided into six groups with five rats in each group. Free PTX solution (dissolved in ethanol/polyoxyethylated castor oil: v/v =1/1) and PTX-loaded liposome formulations (PTX-Lip, PTX-$Asp_1$-Lip, PTX-$Asp_2$-Lip, PTX-$Asp_4$-Lip, and PTX-$Asp_8$-Lip) were intravenous administered to each group at an equivalent dose of 10 mg/kg PTX, respectively. Blood samples (0.5 mL) from the orbit were collected at the predetermined time points (5, 15, 30, 60, 120, 240, 480 and 1440 min) and centrifuged at 5000 rpm for 5 min at 4 °C to obtain the plasma samples. Then, the docetaxel internal standard (10 μL, 50 μg/mL) was added into 100 μL plasma samples, respectively. Extraction was performed with 0.2 mL diethyl ether and the mixture was vortexed for 5 min. After centrifuging at 10 000 rpm for 10 min, the supernatant was dried at 40 °C under a gentle stream of nitrogen in the pressured gas blowing concentrator. Then the dried residue was dissolved in methanol (50 μL) and the mixture was further centrifuged at 10 000 rpm for 10 min. Samples were analyzed by HPLC.

*2.2.9 Biodistribution and targeting bone in vivo*

The evaluation of the bone-targeting ability of these Asp-modified liposomes was performed according to our previous report [Zhao et al., 2019]. In brief, healthy Balb/c mice (18-22 g) were randomly divided

into six groups (n = 5). PTX-Lip, PTX-$Asp_1$-Lip, PTX-$Asp_2$-Lip, PTX-$Asp_4$-Lip, PTX-$Asp_8$-Lip, and the free paclitaxel solution administered via the tail vein at an equivalent dose of 10 mg/kg PTX. 0.5 h, 1 h, 2 h, 4 h, 8 h, 16 h, 24 h after administration, the mice were killed by perfusion. The heart, liver, spleen, lung, kidney, and the lower tibia bone was removed, rinsed with saline, blotted dry, and weighed. Then, to the 100 μL tissue homogenate with twice amount of saline was added 10 μL docetaxel (50 μg/mL) as the internal standard, and the mixture was extracted with 0.2 mL diethyl ether. After vortexing for 5 min, the mixture was centrifuged at 10 000 rpm for 10 min, and the supernatant was dried at 40 °C under a gentle stream of nitrogen in the pressured gas blowing concentrator. Then the dried residue was dissolved in methanol (100 μL) and the mixture was further centrifuged at 10 000 rpm for 10 min. Samples were analyzed by HPLC.

*2.2.10 Statistical analysis*

The concentration efficiency (CE) was used to calculate the bone-targeting capability of liposome. The value of CE was defined as follows: $CE = (C_{max})_L / (C_{max})_P$, where L and P represented the liposomes loading PTX and free PTX, respectively.

All the data were presented as mean ± standard deviation (SD). The statistical analyses were conducted using GraphPad Prism 6.0 (San Diego, CA, USA). Statistical comparisons were performed by analysis of variance (ANOVA) for multiple groups followed by Student's *t*-test. The significance was defined as follows: $^*P < 0.05$, $^{**}P < 0.01$, $^{***}P < 0.001$.

## 3. Results and discussion

### *3.1. Chemistry*

The synthetic procedure of liposome ligand $Asp_8$-Chol was outlined in Scheme 1. The dendritic bone-targeting aspartic acid derivative **8** was synthesized according to our previous described work [Pan et al., 2012]. Briefly, ethyl acrylate **1** and benzylamine **2** underwent a Michael addition reaction at room temperature to obtain the intermediate **3**, which was then hydrogenated, condensated with Boc-Gly-OH, hydrolyzed to generate the core **4**. Subsequently, coupling the core **4** with benzyl protected Asp (Asp(OBn)-OBn) under the EDCI/HOBt to give the first-generation dendritic Asp **5**, which was deprotected in trifluoroacetic acid (TFA) and coupled with the core **4** to obtain the second-generation dendron **7**. Then, the compound **8** was generated by removing the Boc group in TFA. What's more, the acidulated cholesterol derivative **13** was obtained from commercially available cholesterol **9** [Zhao et al., 2019]. Condensation of compound **13** with Asp(OBn)-OBn was conducted in the presence of IBCF/NMM,

followed by the removal of benzyl groups from **14** to give the ligand $Asp_1$-Chol. Subsequently, the $Asp_1$-Chol was coupled with two equivalents of dendron **8** in the presence of IBCF and NMM to generate **15**, which was then debenzylated with 10% Pd/C to give the desired ligand $Asp_8$-Chol.

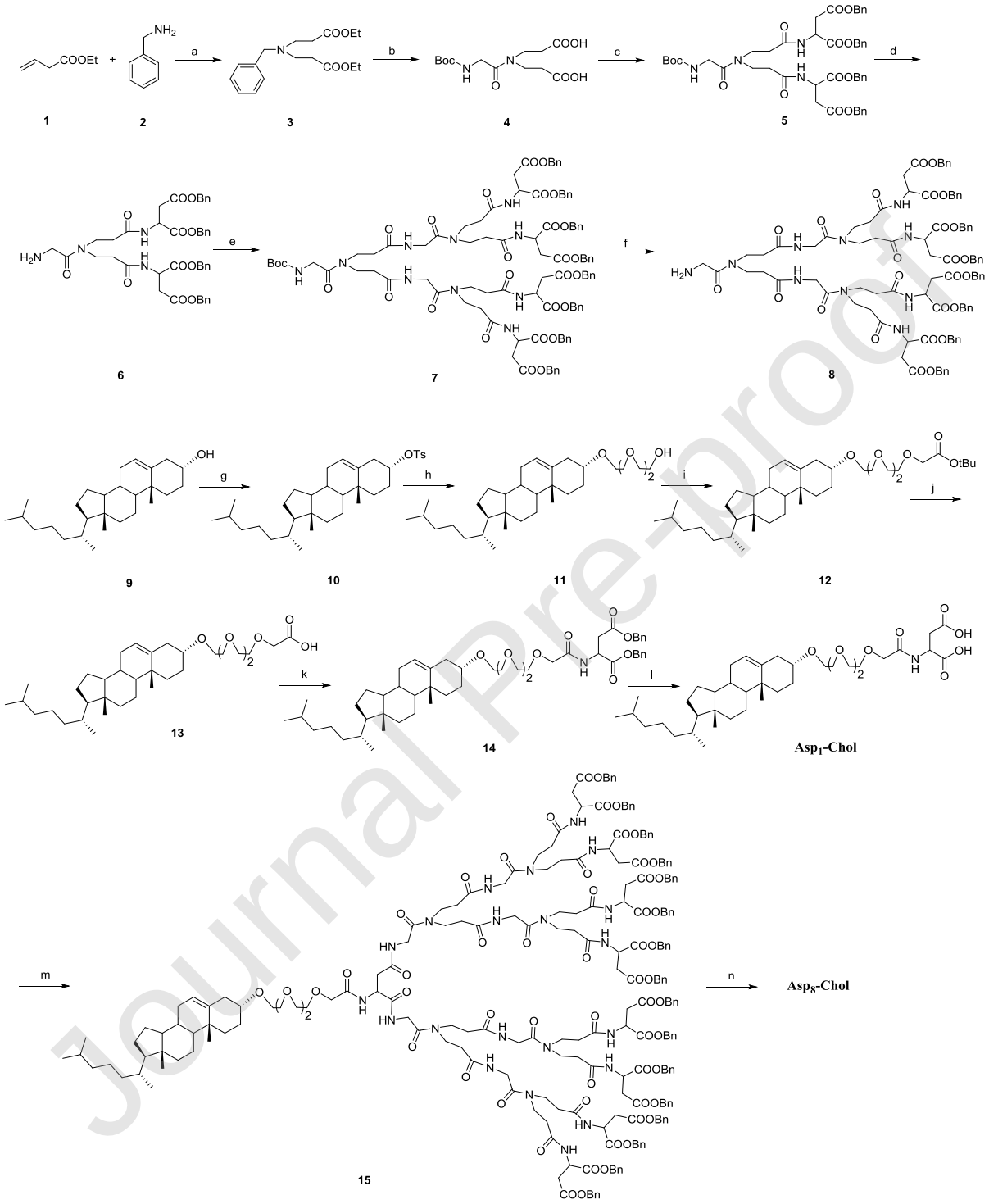


**Scheme 1** Synthesis of ligand $Asp_8$-Chol and $Asp_1$-Chol. Reagents and conditions: (a) $C_2H_5OH$, r.t. (B) i) $HCOONH_4$, Pd/C, $CH_3OH$, r.t.; ii) Boc-Gly-OH, IBCF, NMM, -15 °C - r.t.; iii) NaOH, $H_2O$, r.t. (c) Asp(OBn)-OBn, EDCI, HOBt, $CH_2Cl_2$, r.t.. (d) TFA, $CH_2Cl_2$, r.t. (e) **4**, HBTU, DIPEA, $CH_2Cl_2$, r.t. (f) TFA, $CH_2Cl_2$, r.t. (g) TsCl, pyridine, 50 °C. (h) Triethylene glycol, dioxane, reflux. (i) *t*-butyl bromoacetate, *n*-$Bu_4N^+HSO_4$, 50% NaOH, toluene, r.t. (j) TsOH, tolunene, reflux. (k)

Asp(OBn)-OBn, IBCF, NMM, $CH_2Cl_2$, -15 °C - r.t. (l) $H_2$, Pd/C, $CH_3OH$, r.t. (m) **8**, IBCF, NMM, $CH_2Cl_2$, -15 °C - r.t. (n) $H_2$, Pd/C, $CH_3OH$, r.t.

The synthetic route of ligand $Asp_2$-Chol and $Asp_4$-Chol was shown in Scheme 2. The strategy for synthesis of $Asp_2$-Chol and $Asp_4$-Chol is similar to the preparation of $Asp_8$-Chol. Briefly, the acid **13** was respectively coupled with first-generation dendron **6** or the second-generation dendron **8** utilizing IBCF and NMM as the coupling reagents. Afterwards, the benzyl groups of compound **17** and **16** were removed by catalytic hydrogenolysis to afford $Asp_2$-Chol and $Asp_4$-Chol.

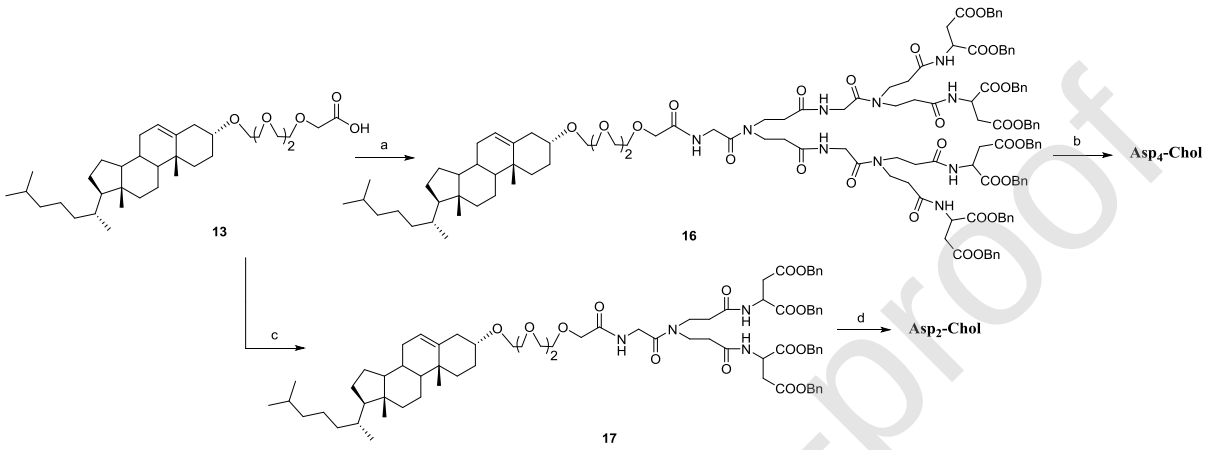


**Scheme 2** Synthesis of ligand $Asp_4$-Chol and $Asp_2$-Chol. Reagents and conditions: (a) **8**, IBCF, NMM, $CH_2Cl_2$, -15 °C - r.t. (b) $H_2$, Pd/C, $CH_3OH$, r.t. (c) **6**, IBCF, NMM, $CH_2Cl_2$, -15 °C - r.t. (d) $H_2$, Pd/C, $CH_3OH$, r.t.

### *3.2. Characterization of liposomes*

PTX-loaded liposomes were prepared by the thin-film hydration method. One of the requirments for liposome to target bone is that they should have proper sizes and uniform distribution [Shi et al., 2015]. As shown in Table 1, the dynamic light scattering results suggested that all the liposomes had the mean diameters about 100-120 nm and low polydispersity index (PDI < 0.24). All the Asp-modified liposomes had the most negative zeta-potential, while the PTX-Lip showed a slightly negative potential. It maybe attribute to the modification with Asp on the liposome's surface, which could increase the net negative charge due to the high density negative carboxyl of Asp and decrease the absorption of the reticuloendothelial system and immune response [Murugan et al., 2015]. The entrapment efficiency were greater than 86%, and drug loading efficiency were about 3%, respectively. All of results contributed to achieve the passive targeting through the enhanced permeability and retention (EPR) effect [Zhang et al., 2009].

**Table 1** The characterization of different PTX-loaded liposomes (n = 3)

| Liposomes | PTX-Lip | PTX-$Asp_1$-Lip | PTX-$Asp_2$-Lip | PTX-$Asp_4$-Lip | PTX-$Asp_8$-Lip |
|---|---|---|---|---|---|
| Size(nm) | 102.7 ± 4.9 | 109.2 ± 3.8 | 106.5 ± 3.3 | 112.4 ± 5.1 | 113.6 ± 4.3 |

| | | | | | |
|---|---|---|---|---|---|
| PDI | 0.192 ± 0.037 | 0.199 ± 0.024 | 0.217 ± 0.019 | 0.232 ± 0.022 | 0.224 ± 0.030 |
| EE (%) | 92.54 ± 3.67 | 92.11 ± 4.87 | 87.46 ± 5.19 | 88.90 ± 3.25 | 86.82 ± 4.34 |
| DL (%) | 3.19 ± 0.17 | 3.11 ± 0.25 | 2.97 ± 0.22 | 3.02 ± 0.27 | 2.94 ± 0.30 |
| Zeta potential (mV) | -1.98 ± 0.27 | -10.42 ± 1.52 | -13.96 ± 2.37 | -15.52 ± 3.96 | -19.33 ± 3.07 |

*In vitro* release studies were used to evaluate entrapment, membrane flexibility and integrity, and affinity of the drug to the carrier systems. In this study, the PTX release behavior from liposomes was evaluated using the dialysis method compared with that of the PTX solution (as control). As shown in Fig. 2A, it was revealed that the PTX solution had a fast release characteristic as more 80% of PTX was released within 10 hours and approximately 100% was released after 24 h. While, the result also showed that PTX-loaded liposomes achieved sustained release behaviors. The PTX-loaded liposome formulations released about 50% of the loaded PTX within 8 hours, and the release exhibited a slow release rate in another 40 hours. What's more, it was worth noting that there was no significant difference between PTX-Lip, PTX-Asp$_1$-Lip, PTX-Asp$_2$-Lip, PTX-Asp$_4$-Lip, and PTX-Asp$_8$-Lip on the release property. And none of the PTX-loaded liposomes displayed burst initial release patterns. All the results indicated that dendritic aspartic acid modification on the surface of liposome didn't change the release profile of PTX.

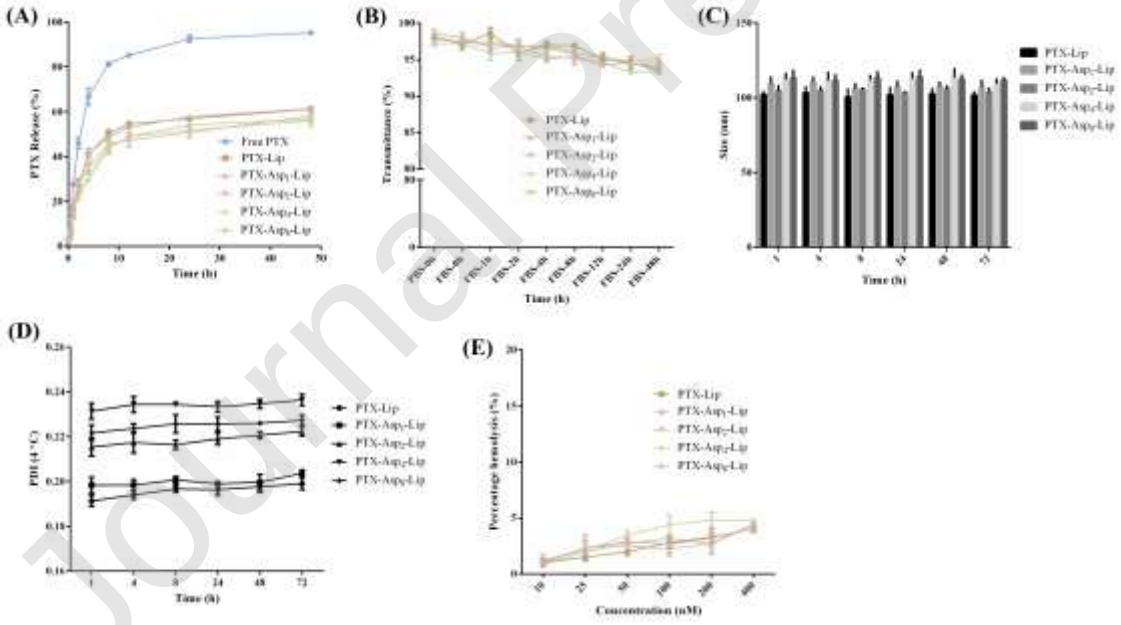


**Figure 2**. In vitro characterization of PTX-loaded liposomes. (A) The PTX release profiles of free PTX, PTX-Lip, PTX-Asp$_1$-Lip, PTX-Asp$_2$-Lip, PTX-Asp$_4$-Lip, and PTX-Asp$_8$-Lip in PBS containing 0.1% Tween 80. (B) The variations of transmittance of different modified liposomes in 50% FBS. (C) Size at 4 $^{o}$C for three days. (D) PDI at 4 $^{o}$C for three days. (E) Hemolysis percentage of different liposomes. (n = 3, mean ± SD)

Liposomal particle stability against physiological condition is prerequisite for the further application *in vivo* [Taira et al., 2004]. The turbidity variations of different liposomes were measured to investigate the

stability of liposomes in serum. As shown in Fig. 2B, the transmittances of all the liposomes were over 90% and these liposomes didn't show obvious change within 48 h cultured with FBS, which suggested that no aggregation or sediment was appeared. On the other hand, the results of physical stability was shown in Fig 2C and 2D. The average size was almost unchanged at 4 ℃ for three days (Fig. 2C), and PDI increased slightly (Fig. 2D). All the results implied that the liposomes were sufficient serum stability and physical stability, which is important for obtaining a longer half-life of blood *in vivo*.

The hemocompatibility of the Asp-modified liposomes drug delivery system was evaluated using the e erythrocyte hemolysis test. As expected, hemolysis assay of PTX-loaded liposomes demonstrated that the five types of liposomes did not show any significant increase in the hemoglobin release with up to 400 nM of phospholipids (Fig. 2E) and concentration-dependent increase in hemolysis (< 5% hemolysis rate was regarded as non-toxic) [Li et al., 2018], which suggested that they had a good biosecurity.

### *3.3. HAP binding assay*

As shown in Fig. 3, all the liposomes exhibited some HAP affinity, whereas the free paclitaxel was at best negligibly bound. Moreover, compared with the uncoated liposome PTX-Lip, the Asp-modified liposomes showed dramatic binding rates. It was also revealed in Fig. 2 that the HAP binding efficiency was increased in a time-dependent manner. And the more Asp on the surface of liposomes, the stronger the HAP binding ability. These results demonstrated that dendritic Asp-modified liposomes had good bone-targeting ability, and facilitated the next *in vivo* experiments.

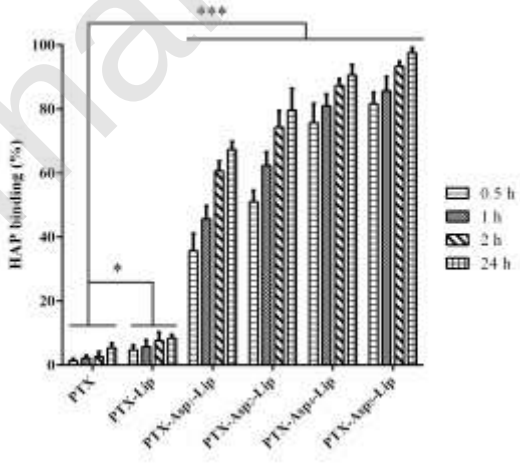


**Figure 3**. Percentage of PTX from each formulation bound to HAP. *P < 0.05, ***P < 0.001. (n = 3, mean ± SD)

### *3.4. Cytotoxicity assay*

In spite of extensive applicability in biological system, the use of dendron for liposomal drug delivery is constrained due to its inherent toxicity. Surface engineering, including PEGylation, amino acids

conjugation and peptide conjugation, is one of the most effective ways to improve the biocompatibility of dendron [Pan et al., 2012]. In this study, natural amino acids were chosen to modify liposome for bone-targeting. Fig. 4 showed the MTT assay results of cytotoxicity of blank liposomes against MDA-MB-231 cells. As expected, the results suggested that the PTX-unloaded formulations didn't show significant cytotoxicity at different concentrations (0.64-2000 ng/mL), and >90% of MDA-MB-231 cells survived. As a summary, all the unloaded formulations, especially the synthetized aspartic acid dendrons, were non-toxic or low-toxic in the tested concentrations.

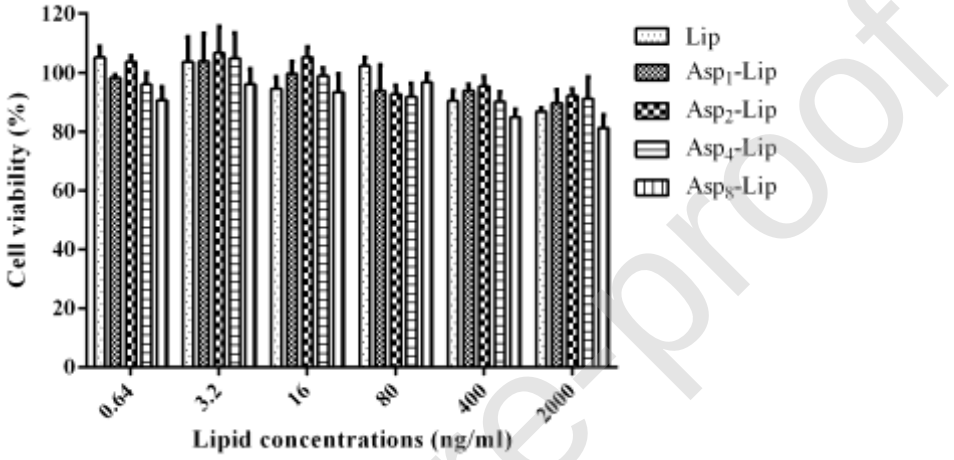


**Figure 4**. Cytotoxicity of unloaded liposomal formulations (n = 3, mean ± SD)

### *3.5. Pharmacokinetic studies*

For pharmacokinetic study, the HPLC analytical method was established and validated as our previous report [Zhao et al., 2019]. The pharmacokinetic profiles of paclitaxel from PTX-loaded liposomal formulations and PTX solution were compared by measuring the concentration of PTX in rat plasma after administration at 10 mg/kg. The main pharmacokinetic parameters were analyzed by DAS 2.0. As shown in Fig. 5 and Table 2, the concentration of PTX released from each liposome (PTX-Lip, PTX-$Asp_1$-Lip, PTX-$Asp_2$-Lip, PTX-$Asp_4$-Lip, and PTX-$Asp_8$-Lip) was much higher than that of naked PTX. But there were no significant differences between these liposomal formulations. It was also outlined that the liposomes could increase the area under the concentration-time curve ($AUC_{0-t}$) of PTX within 24 h compared with the PTX solution group. What's more, the Asp-modified liposomes could extend the elimination half-life ($t_{1/2}$) of free PTX from 247 min to 395 min ($p < 0.01$). All the results indicated that the targeted liposomes might be temporarily restored in the plasma and slowly dissociate from the contents in plasma, and this consequently lead to the superior circulation time of modified liposomes *in vivo*.

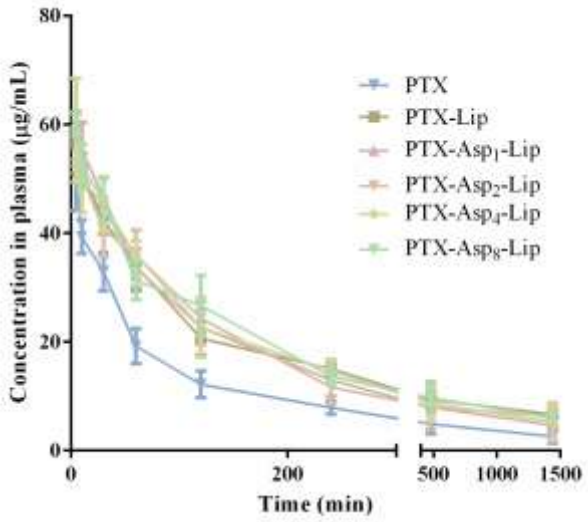


**Figure 5**. Plasma concentrations of paclitaxel in normal SD rats of different PTX formulations (n = 5, mean ± SD).

**Table 2**. The pharmacokinetic parameters of different PTX formulations. **P < 0.01. (n = 5, mean ± SD)

| | $AUC_{(0-t)}$ (μg/mL·min) | $C_{max}$ (μg/mL) | $t_{1/2}$ (min) |
|---|---|---|---|
| PTX | 8537.99 ± 1547.26 | 50.37 ± 5.10 | 247.52 ± 19.88 |
| PTX-Lip | 12589.47 ± 1787.52** | 56.67 ± 4.64 | 343.29 ± 46.19** |
| PTX-$Asp_1$-Lip | 13547.61 ± 2086.11** | 56.44 ± 2.94 | 367.11 ± 39.84** |
| PTX-$Asp_2$-Lip | 13375.65 ± 1439.23** | 57.67 ± 3.39 | 371.58 ± 49.63** |
| PTX-$Asp_4$-Lip | 13586.48 ± 1756.36** | 59.21 ± 7.79 | 382.47 ± 51.67** |
| PTX-$Asp_8$-Lip | 13995.76 ± 1883.61** | 60.00 ± 1.63 | 395.87 ± 58.91** |

### *3.6. Biodistribution and targeting bone in vivo*

The biodistribution study was conducted in healthy Balb/c mice to determine whether there was preferential targeting of the dendritic Asp-modified liposomes to bone in *vivo*. The paclitaxel was quantified in each organ and calculated as the percentage of administrated dose per gram of tissue (%AD·$g^{-1}$). As shown in Fig. 6, it was observed that a considerable amount of PTX from paclitaxel solution was accumulated in the heart (Fig. 6A) and kidney (Fig. 6E) at 2 h post-administration. While, the uptake was reduced by a factor of five (heart) and a factor of seven (kidney) respectively after 8 h. What's more, it should be worth noting that there was a relatively lower drug uptake in other organs (Fig. 6B, 6C, 6D), especially in lower tibia bone (Fig. 6F).

For all the liposome formulations, it was shown that both liver and spleen had significant uptake in these groups (Fig. 6B, 6C). Liver and spleen are considered to be the major macrophage organs, and thus the intravenously injected liposomes were eliminated rapidly through the two organs. The uptake of

Asp-modified liposomes groups in liver was 10% and spleen was about 15% respectively at 2 h post-administration. But, there was no significant difference between these groups. It was also found that the uptake of other organs (heart, lung, and kidney) were also more consistent between the dendritic aspartic acid modified liposomes groups (Fig. 6A, 6D, 6E). Interestingly, the Fig. 6F showed that there was a significant accumulation in lower tibia bone in the Asp-modified liposomes groups attributing to the bone targeting ability of aspartic acid. All the PTX-loaded liposomes reached the maximum distribution in the bone lesion at 2 h after injection. Especially, the concentration efficiencies (CEs) of PTX-$Asp_8$-Lip, PTX-$Asp_4$-Lip, PTX-$Asp_2$-Lip, PTX-$Asp_1$-Lip, PTX-Lip were enhanced to 4.65 ($p < 0.001$), 3.56 ($p < 0.001$), 2.85 ($p < 0.01$), 2.31 ($p < 0.01$), 1.97 ($p < 0.01$) times higher than that of free PTX group. And it is worth noting that it showed an increasing trend with the increase of the number of aspartic acid residues. So these data further proved our conjecture that all the ligand-modified liposomes can deliver paclitaxel to the bone lesions, which had a descending trend as PTX-$Asp_8$-Lip > PTX-$Asp_4$-Lip > PTX-$Asp_2$-Lip > PTX-$Asp_1$-Lip > PTX-Lip. Moreover, the more quantity of Asp residues exposed to the liposome surface, the more paclitaxel delivered to bone, which means the stronger affinity to bone. Therefore, the PTX-$Asp_8$-Lip showed the best affinity, which was consistent with the result of the HAP binding assay. These results provided a novel and effective entry to the development of bone-targeting drugs.

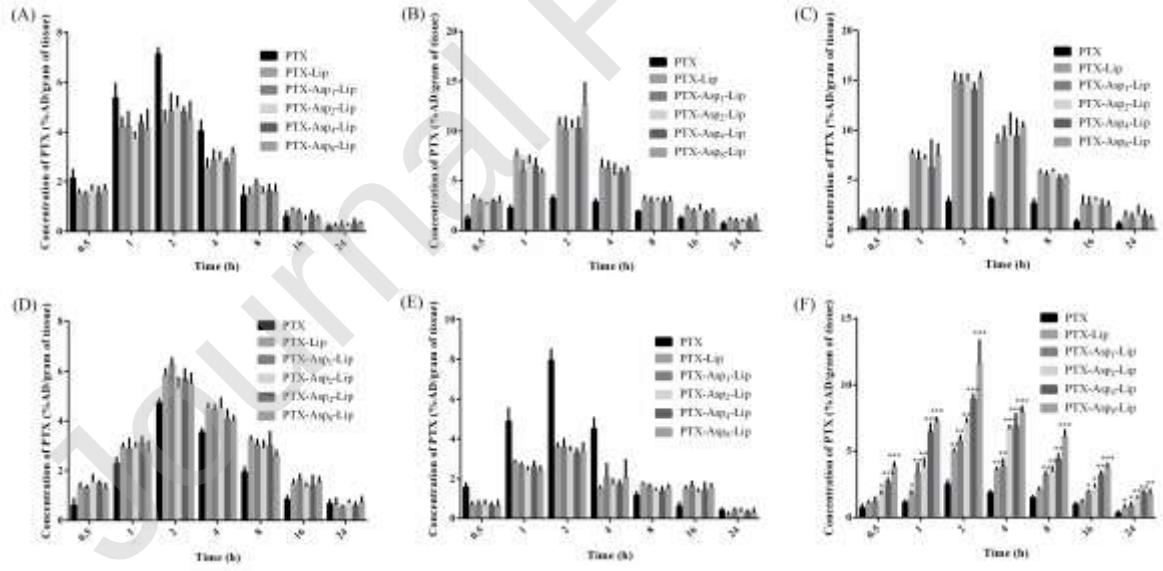


**Figure 6.** In vivo distribution of PTX after injection of free PTX, PTX-Lip, PTX-$Asp_1$-Lip, PTX-$Asp_2$-Lip, PTX-$Asp_4$-Lip, and PTX-$Asp_8$-Lip. (A) heart, (B) liver, (C) spleen, (D) lung, (E) kidney, (F) bone. *P < 0.05, **P < 0.01, ***P < 0.001. (n = 5, mean ± SD)

## 4. Conclusion

In this study, we have designed and successfully synthesized a series of novel dendritic aspartic acid derivatives with high affinity as ligands for bone targeting liposomes. These liposomes possess good biosecurity and high HAP binding efficiency *in vitro*. What's more, the bone-targeting study *in vivo* suggested that all liposomes could increase the accumulation of PTX in bone, among which, the PTX-$Asp_8$-Lip showed the best affinity due to the more aspartic acid residues exposed on the liposome surface. Generally, this work presented a way that the synthesis of liposome ligand may be used as potential means to improve the therapeutic efficiency in bone diseases.

## Conflict of interest

The authors declare no competing financial interest.

## Acknowledgement

This work was supported by the National Natural Science Foundation of China (No.81903448).

### References

Chastain, D.B., Davis, A., 2019. Treatment of chronic osteomyelitis with multidose oritavancin: A case series and literature review. Int. J. Antimicrob. Ag. 53, 429-434.

Li, Y.M., Lin, J.T., Zhi, X.L., Li, P.F., Jiang, X.F., Yuan, J., 2018. Triple stimuli-responsive keratin nanoparticles as carriers for drug and potential nitric oxide release. Mat. Sci. Eng. C-Mater. 91, 606-614.

Matsuo, M., Ohyama, S., Sakurai, K., Toyota, T., Suzuki, K., Sugawara, T., 2019. A sustainable self-reproducing liposome consisting of a synthetic phospholipid. Chem. Phys. Lipids. 222, 1-7.

Murugan, K., Choonara, Y.E., Kumar, P., Bijukumar, D., du Toit, L.C., Pillay, V., 2015. Parameters and characteristics governing cellular internalization and trans-barrier trafficking of nanostructures. Int. J. Nanomed. 10, 2191-2206.

Pan, J.Z., Guo, L., Ouyang, L., Yin, D.Q., Zhao, Y., 2012. Synthesis, Antibacterial Activity and Cytotoxicity of Novel Janus Peptide Dendrimers. Synlett, 23, 1937-1940.

Pan, J.Z., Wen, M., Yin, D.Q., Jiang, B., He, D.S., Guo, L., 2012. Design and synthesis of novel amphiphilic Janus dendrimers for bone-targeted drug delivery. Tetrahedron 68, 2943-2949.

Sarig, S., 2004. Aspartic acid nucleates the apatite crystallites of bone: ahypothesis. Bone 35, 108-113.

Shi, K.R., Li, J.P., Cao, Z.L., Yang, P., Qiu, Y., Yang, B., Wang, Y., Long, Y., Liu, Y.Y., Zhang, Q.Y., Qian, J., Zhang, Z.R., Gao, H.L., He, Q., 2015. A pH-responsive cell-penetrating peptide-modified liposomes with active recognizing of integrin αvβ3 for the treatment of melanoma. J. Control. Release 217, 138-150.

Sun, W., Ge, K., Jin, Y., Han, Y., Zhang, H., Zhou, G., Yang, X., Liu, D., Liu, H., Liang, X.J., Zhang, J., 2019. Bone-Targeted Nanoplatform Combining Zoledronate and Photothermal Therapy To Treat Breast Cancer Bone Metastasis. ACS Nano 13, 7556-7567.

Taira, M.C., Chiaramoni, N.S., Pecuch, K.M., Alonso-Romanowski, S., 2004. Stability of liposomal formulations in physiological conditions for oral drug delivery. Drug Deliv. 11, 123-128.

Yamashita, S., Katsumi, H., Hibino, N., Isobe, Y., Yagi, Y., Tanaka, Y., Yamada, S., Naito, C., Yamamoto, A., 2018. Development of PEGylated aspartic acid-modified liposome as a bone-targeting carrier for the delivery of paclitaxel and treatment of bone metastasis. Biomaterials 154, 74-85.

Zhang, L., Yu, F.Q., Cole, A.J., Chertok, B., David, A.E., Wang, J.K., Yang, V.C., 2009. Gum Arabic-Coated Magnetic Nanoparticles for Potential Application in Simultaneous Magnetic Targeting and Tumor Imaging. AAPS J. 11, 693-699.

Zhao, Y., He, D.S., Ma, L.F., Guo, L., 2015. Synthesis and Preliminary Evaluation of Novel Bone-targeting NSAIDs Prodrugs based on Glutamic Acid Oligopeptides. Lett. Drug Des. Discov. 12, 585-590.

Zhao, Y., Qu, B.Y., Wu, X.Y., Li, X.C., Liu, Q.Q., Jin, X.X., Guo, L., Hai, L., Wu, Y., 2014. Design, Synthesis and biological evaluation of Brain Targeting L-Ascorbic Acid Prodrugs of Ibuprofen with "Lock-in" function. Eur. J. Med. Chem. 82, 314-323.

Zhao, Y., Zhang, L., Peng, Y., Yue, Q.M., Hai, L., Guo, L., Wang, Q.T., Wu, Y., 2018. GLUT1-mediated venlafaxine-thiamine disulfide system-glucose conjugates with “lock-in” function for central nervous system delivery. Chem. Biol. Drug Des. 91, 707-716.

Zhao, Z., Zhao, Y., Xie, C.W., Chen, C.Q., Lin, D., Wang, S., Lin, D., Cui, X.H., Guo, Z.S., Zhou, J.F., 2019. Dual-active targeting liposomes drug delivery system for bone metastatic breast cancer: synthesis and biological evaluation. Chem. Phys. Lipids. 223, 104785.